Continuous formation of localized moment in Ir-Pt(Fe)

T. Takabatake, H. Mazaki, and T. Shinjo
Institute for Chemical Research, Kyoto University, Kyoto, Japan
(Received 1 October 1981)

Mössbauer measurements of ^{57}Fe impurities in $Ir_{1-x}Pt_x$ ($0 \leq x \leq 0.50$) alloys have been performed at temperatures in the range 1.5 to 40 K in external magnetic fields up to 80 kOe. From each spectrum the distribution of effective hyperfine field was derived. Then the distribution curve was decomposed into components characterized by the number of Pt nearest neighbors N. As N increases from 0 to 9 the temperature and field dependences of the hyperfine field shift continuously. These dependences are appreciably affected by the difference in the number of next-nearest Pt neighbors. The results indicate that the magnetic state of Fe impurities in Ir-Pt hosts changes smoothly from the localized spin fluctuation state to the giant moment state with the aid of polarization of nearest and also next-nearest Pt neighbors.

I. INTRODUCTION

The problem of local moment formation of dilute impurities in paramagnetic binary alloys has been extensively investigated.[1] Mössbauer study in this field has been concentrated upon the Nb-Mo(Fe) system,[2–5] because the magnetic character of Fe impurities in the constituent elements has been well known. Earlier experiments on the system[2–4] qualitatively supported the model of Jaccarino and Walker.[6] According to the model, the moment formation is a discontinuous process where the Fe impurity carries a full moment if surrounded by 7 or 8 Mo nearest neighbors (NN's). However, the latest experiment by Maley *et al.*[5] indicates that the magnetic behavior of Fe impurity depends more continuously on the NN configuration. This result is in agreement with the model recently proposed by van der Rest,[7] where the magnetic moment is built up smoothly depending both on NN configuration and on host composition. In addition, it is pointed out that the moment induced on NN atoms is essential to the moment per impurity when NN atoms have a large magnetic susceptibility.

In the present paper, we report a Mössbauer study of Ir-Pt(Fe) alloys. Ir(Fe) is not a simple nonmagnetic system such as Nb(Fe), but a localized spin fluctuation (LSF) system with an LSF temperature of 225 K.[8] The hyperfine field of ^{57}Fe in Ir is much smaller than those of usual Kondo systems and the saturation hyperfine field increases in proportion to the external field up to 80 kOe.[9,10] On the other hand, Pt(Fe) shows a free spin behavior of the giant magnetic moment of $6.46\mu_B$ at temperatures above 4 K,[11] and the Kondo temperature is far below 0.1 K.[12] From magnetic-susceptibility measurements of $(Ir_{1-x}Pt_x)_{0.99}Fe_{0.01}$, Geballe *et al.*[13] showed that the effective magnetic moment per Fe atom changes from $0.53\mu_B$ ($x=0$) to $6.2\mu_B$ ($x=1$).

Mössbauer study of the ternary alloy system $Ir_{1-x}Pt_x$(Fe) is therefore expected to give microscopic information about the transition process from the LSF state to the giant moment state. Ir and Pt metals form a series of solid solutions having the fcc structure. An Fe impurity atom at regular lattice site of Ir-Pt alloys has 12 NN's and 6 NNN's. Since Ir and Pt have a large photon cross section for 14.4-keV Mössbauer γ rays of ^{57}Co, the source technique is more effective than the absorber technique. In addition, the source technique has the advantage that one can use a sample with extremely low impurity concentrations.

II. EXPERIMENTAL

A. Sample preparation

Mössbauer sources of $Ir_{1-x}Pt_x$(^{57}Co) ($x=0, 0.05, 0.10, 0.17, 0.30, 0.50$) were prepared by diffusing ^{57}Co into host alloys. The host alloys except for $x=0$ were arc cast from high-purity elements. As a host of $x=0$, a 50-μm Ir foil (99.99% pure) was used. Appropriate amounts of Ir and Pt metals (99.99% pure, 100-mesh powder) were melted in a cold copper crucible under Ar atmosphere. The alloys were annealed at 1100 °C for 7d, and then sliced off into disks of about 0.3 mm thickness and 9 mm diameter. Onto the disk area of 35 mm^2, 0.4–2 mCi of ^{57}Co was electrodeposited from an ammoniacal solution. Diffusion was carried out at 1400 °C for 5 h in a mixed atmosphere of H_2 and Ar. The disks were subsequently cooled to room temperature at a rate of 600 °C/h. The surface was chemically etched in a dilute solution of HCl and HNO_3. In order to avoid precipitation, each sample was again heat treated at a

temperature higher by 100 °C than the miscibility temperature.[14] The sample was sealed in a quartz capsule under a partial pressure of Ar. After heat treatment for 3 h, the sample was rapidly quenched into water. Finally, the surface was again chemically etched.

Assuming the average depth of diffusion is 20 μm, the average concentration of ^{57}Co corresponds to 10–50 atomic ppm depending on the amount of electrodeposited ^{57}Co. The composition of host alloys was approximated by the known initial weights of constituent elements.

B. Apparatus and measurements

Mössbauer measurements were performed in a longitudinal geometry with a fixed cold source and a moving room-temperature absorber. A schematic of the Dewar system with the spectrometer is shown in Fig. 1. The sample was mounted in the superconducting magnet capable of attaining fields up to 80 kOe. The magnet was operated in a persistent current mode. The axis of field was perpendicular to the sample surface and was parallel to the γ-ray direction. Temperatures below 4.2 K were obtained by pumping down the inner cell of the sample holder, into which liquid He distills from the He bath through a needle valve. Sample temperature was measured and regulated to better than ±0.05 K between 1.5 and 40 K using a calibrated carbon glass resistor and a temperature controller. Although the resistor is slightly field sensitive, the effect was corrected by means of a field insensitive thermocouple, Au–0.07 at.% Fe vs Ag–0.37 at.% Au.

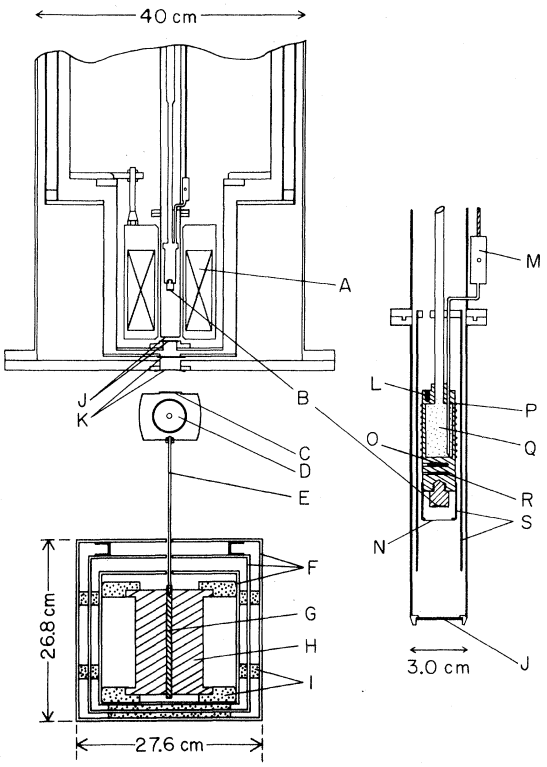

FIG. 1. Dewar system and spectrometer for high-field Mössbauer measurement. A: superconducting magnet; B: sample (^{57}Co in Ir-Pt); C: absorber (potassium ferrocyanide); D: proportional counter; E: Al rod; F: magnetic shield case, G: drive rod; H: velocity transducer; I: Bakelite spacers; J: Be windows; K: Mylar windows; L: carbon resistor thermometer; M: needle valve; N: Al foil; O: carbon glass resistor thermometer; P: heater, Q: Cu chips; R: thermocouple (Au–0.07 at.% Fe vs Ag–0.37 at.% Au); S: Cu radiation shields.

As a single line absorber, potassium ferrocyanide containing 1.0 mg/cm^2 of ^{57}Fe was used. In the arrangement of Fig. 1, the fringing field acting on the absorber is about 3% of the field at the magnet center, resulting in a broadening of the line width.

Measuring period for a spectrum is 14–58 h. Longer periods were required for samples with higher Pt concentration, because they give low counting rates and poor signal/noise ratios resulting from the larger diffusion depth of ^{57}Co.

In a high field, say 80 kOe, the effect of stray field on the velocity transducer becomes serious.[10] To avoid this, a magnetic shield case was prepared. As shown in Fig. 1, the shield case consists of three boxes; the outer is made of pure Fe, the middle by $Fe_{55}Ni_{45}$, and the inner by $Fe_{22}Ni_{78}$(Mo,Cu). When the external field of 80 kOe is applied, the stray field at the top of the case is 260 Oe. Inside the case, however, the field is reduced to less than 1 Oe, which permits us to neglect the effect on the transducer. Thus, velocity calibration was made with the known magnetic splitting of α-Fe under zero field.

III. RESULTS AND DISCUSSION

Prior to discussing spectra obtained under external magnetic fields, we present the result in zero field. The values of isomer shift (IS) and of full width at half-maximum (FWHM) were evaluated by fitting the spectrum to a Lorentzian shaped line. Table I lists the results obtained using an absorber of potassium ferrocyanide containing 0.5 mg/cm^2 of ^{57}Fe, which has 0.34-mm/s FWHM against a Rh(^{57}Co) source (New England Nuclear).

As shown in the table, FWHM increases with Pt concentration. The broadening is exclusively attributed to the distribution of IS of ^{57}Fe impurities with various neighbors. Somewhat large line width for $x=0$ may be due to inhomogeneity caused by the omission of the fast quenching procedure in the sample preparation. At the lowest temperature 1.5 K, additional line broadenings for any x are less than 6% of the value at 290 K, indicating that no spontaneous

TABLE I. Summary of results at room temperature in zero field for sources of ^{57}Co diffused into $Ir_{1-x}Pt_x$ hosts. IS is the isomer shift relative to α-Fe, FWHM is the experimental line width against a $K_4[Fe(CN)_6]\cdot 3H_2O$ absorber containing 0.5 mg/cm^2 of ^{57}Fe.

$Ir_{1-x}Pt_x$ x	IS (mm/s)	FWHM (mm/s)
0	−0.261	0.378
0.05	−0.278	0.334
0.10	−0.287	0.357
0.17	−0.308	0.393
0.30	−0.321	0.421
0.50	−0.341	0.445

magnetic ordering occurs down to 1.5 K.

In Fig. 2, IS at temperatures of 290 and 4.2 K is plotted as a function of Pt concentration, where IS is for sources and hence more negative shifts correspond to a decrease in electron density at ^{57}Fe nucleus. The figure shows that the electron density gradually decreases as Pt concentration increases.

High-field Mössbauer measurements were performed in external magnetic fields H_{ext} up to 80 kOe between 1.5 and 40 K. In the presence of H_{ext}, the ^{57}Fe nucleus feels an effective magnetic field H_{eff}, i.e., $H_{eff}=H_{ext}+H_{hf}$. The magnitude of hyperfine field H_{hf} depends on the local environment of the Fe impurity. In random Ir-Pt alloys, the probability that an Fe atom has N NN Pt atoms is given by the appropriate binominal distribution.

Figure 3(a) shows a typical set of spectra obtained at 4.2 K and 80 kOe, where solid lines are deduced

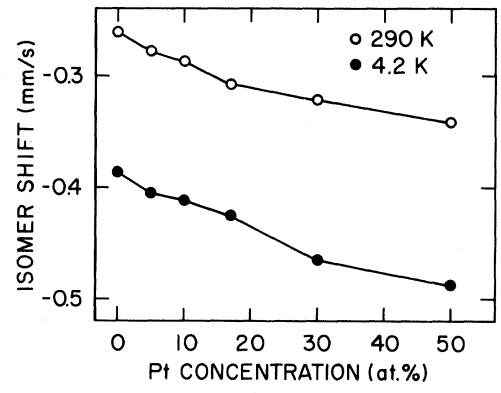

FIG. 2. Isomer shift of ^{57}Fe in $Ir_{1-x}Pt_x$ hosts as a function of Pt concentration. Shifts are given with respect to α-Fe, where isomer shifts are for sources (rather than absorbers) and hence more negative shifts correspond to a decrease in electron density at ^{57}Fe nucleus.

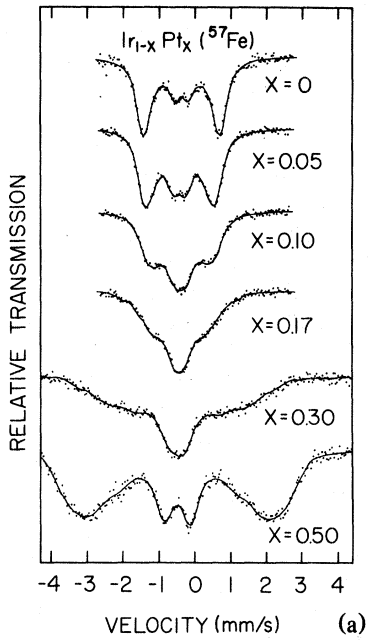

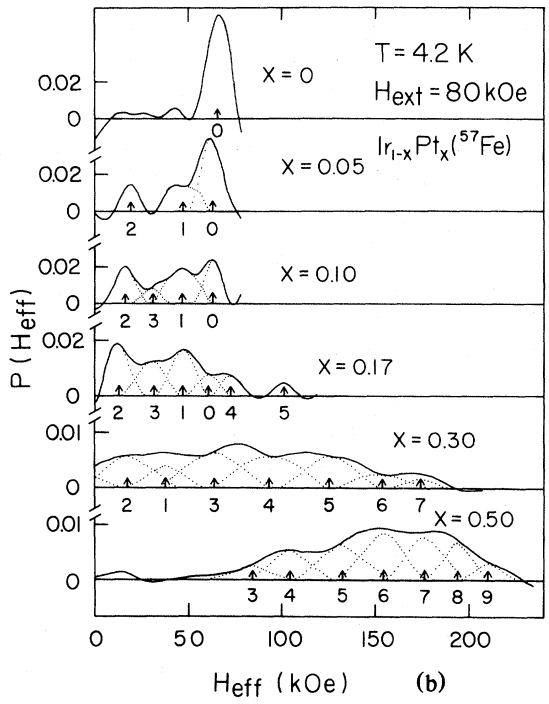

FIG. 3. (a) Mössbauer spectra of $Ir_{1-x}Pt_x(^{57}Fe)$ in a longitudinal field of 80 kOe at 4.2 K. Solid lines are the fits with effective hyperfine field distributions presented in (b) (see text). (b) Effective hyperfine field distribution derived from the spectra in (a). Solid lines are obtained by means of the smoothed histogram method. Dotted lines indicate decomposed components of Fe atoms with N nearest-neighbor Pt atoms. Arrows mark the mean effective hyperfine field of the component characterized by N.

from the analysis of the distribution of effective field (see below). These spectra depend remarkably on Pt concentration. Slight asymmetry in the spectra is mainly due to the distribution of IS.

Analysis of these spectra was made by two distinct methods; one is based on the model of discontinuous moment formation, and the other allows a continuous moment formation. First, in accordance with the discontinuous model, we tried to fit the spectra using two components, i.e., high-field (magnetic) and low-field (nonmagnetic or weakly magnetic) components. It is assumed that each component consists of four Lorentzian lines with the ideal intensity ratio of 3:0:1:1:0:3 and equal line widths. The peak position and line width of each component are treated as free parameters. In Table II are listed the parameters analyzed for $x=0.05$, 0.10, and 0.17, but the spectra of $x=0.30$ and 0.50 could not be well fitted by this method.

The features derived from two-component fitting are as follows: (1) H_{hf} of each component is not independent of Pt concentration x. As to the low-field component, H_{hf} varies from -15.0 to -28.6 kOe when x changes from 0 to 0.17. (2) The line width of the low-field component increases rapidly with Pt concentration. (3) As listed for the samples of $x=0.05$ and 0.10, comparison of relative areas of two components with the probabilities of binominal distribution suggests that Fe atoms with 0 or 1 Pt NN's correspond to the low-field component, and those for $N\geq 2$ to the high-field component. This suggestion cannot account for $x=0.17$, where relative area for the high-field component is 0.45, being much smaller than the statistical probability 0.63. This discrepancy cannot be explained even by taking into account the effect of NNN Pt atoms, because they enhance the probability of high-field component, but do not suppress it.

Above characteristics suggest that the discontinuous model is not appropriate to understand our data, i.e., the spectra are not composed of two components with distinct H_{eff}, but are superposition of widely distributed H_{eff}. Based on this fact, we next attempt to obtain the distribution of effective field $P(H_{eff})$ in two ways; one is the Fourier-series method developed by Window[15] and the other is the smoothed histogram method by Hesse and Rübartsch.[16] These methods have been successfully applied for the analysis of broad, overlapping spectra of binary alloys such as Cu-Fe and Fe-V.[17,18] In our analysis, the distribution of IS is taken into account by supposing that the shift in IS is in proportion to H_{hf}. The maximum (cutoff) field is properly chosen so as to see no peaks beyond the field. When both methods present similar $P(H_{eff})$ curves, we adopt it as a reliable result.

In Fig. 3(b) are shown $P(H_{eff})$ curves determined by the smoothed histogram method. Negative values appeared in the figure are probably caused by an unphysical oscillation related with the analysis method.[16] The figure clearly shows that the curves do not consist of two distinct peaks with fixed positions expected from the discontinuous model, but have more complex profiles and are widely distributed especially for $x=0.30$ and 0.50. From the curves, the spectra given by the full lines in Fig. 3(a) are obtained.

In order to analyze $P(H_{eff})$ curves, it is assumed that Ir and Pt atoms are distributed randomly and that H_{hf} of ^{57}Fe impurity is mainly correlated to the configuration of NN shell. We discuss below in some detail the procedure how to decompose $P(H_{eff})$ curves into components characterized by the number of NN Pt atoms.

(i) First, we treat $x=0.05$. Comparing the curve with that of $x=0$, it appears that the main peak for $x=0.05$ corresponds to Fe atoms with zero Pt NN. The isolated peak at around 19 kOe can be attributed either to the component for $N=1$ or to 2, but the relative peak intensity supports that this peak comes from $N=2$. Note that the mean value of H_{hf} for $N=2$ cannot be determined uniquely, because in the presence of H_{ext} the sign of H_{eff} is unknown ($H_{hf}=-80\pm 19=-61$ or -99 kOe). Subtracting the peak of $N=0$, one can emboss the component of $N=1$, given by the dotted line in the figure. The configurations of $N\geq 3$ are of negligible probabilities (<0.02).

TABLE II. Summary of parameters obtained by the trial fitting of the spectra in Fig. 3(a) using two components with distinct H_{eff}. For $x=0.30$ and 0.50, the spectra could not be well fitted by this method. N is the number of Pt nearest neighbors.

	Low-field component				High-field component			
$Ir_{1-x}Pt_x$ x	H_{hf} (kOe)	FWHM (mm/s)	Relative area	Probability for $N=0,1$	H_{hf} (kOe)	FWHM (mm/s)	Relative area	Probability for $N\geq 2$
0	−15.0	0.529						
0.05	−21.4	0.549	0.82	0.882	−58.2	0.617	0.18	0.118
0.10	−26.5	0.657	0.64	0.659	−63.7	0.655	0.36	0.341
0.17	−28.6	0.728	0.55	0.370	−67.2	0.645	0.45	0.630

(ii) From the assumption of binominal distribution, $P(H_{\text{eff}})$ curve of $x=0.10$ is expected to include another component of $N=3$ with the intensity of 0.085. This component is brought out by subtracting the peaks of $N=0$, 1, and 2 from the total curve. As pointed out in (i), H_{hf} for $N=2$ has two possible values, -64 and -96 kOe, but the fact that the absolute value of H_{hf} for $N=3$ should be larger than that for $N=2$ gives $H_{\text{hf}}=-111$ kOe for $N=3$.

(iii) For $x=0.17$, we notice two other peaks. The peak near 73 kOe is identified as the component of $N=4$ and the isolated peak near 101 kOe is considered to be the component of $N=5$. Similar to (i) and (ii), H_{hf} for $N=2$ is -67.5 or -92.5 kOe. However, assuming that the absolute value of H_{hf} increases with Pt concentration, one can reasonably choose at this stage that $H_{\text{hf}}(N=2)=-61$, -64, and $-67,5$ kOe for $x=0.05$, 0.10, and 0.17, respectively.

(iv) As to $x=0.50$, the symmetry in the probability of binominal distribution with respect to $N=6$ makes the analysis easier than the case of $x=0.30$. Thus, peaks of $N=3-9$ were generated so as to fit to the total curve. The probability of other N can be ignored.

(v) The gently sloping feature of the curve for $x=0.30$ makes the analysis difficult. The result of $x=0.50$ gives a clue towards the determination of peak positions for $N=7-5$. We therefore started the decomposition with $N=7$ and successively proceeded to $N=1$. H_{hf} of $N=2$ was determined as -97 kOe in accordance with the assumption that H_{hf} increases with Pt concentration.

Decomposed peaks in Fig. 3(b) reveal that both position and width of each component depend on x, i.e., the mean value as well as the width of H_{hf} increase with Pt concentration. A remarkable change occurs between $x=0.17$ and 0.30. This tendency can be explained by the difference in the number of NNN Pt atoms $M(\leq 6)$. For example, the probability of $M\geq 3$ remarkably increases from 0.066 to 0.256 in the range of $x=0.17-0.30$. Increase of M inevitably results in the enhancement of H_{hf}. In addition, various configurations of NNN shells become possible, and this yields the broadening of H_{hf}.

In Fig. 4, H_{hf} is plotted as a function of N. The value for $N=12$ is derived from the data on Pt(Fe).[11] The figure shows that H_{hf} increases rather smoothly with increasing N and that relatively sharp increase in H_{hf} occurs between $N=2$ and 3. As discussed before, the dispersion in H_{hf} for $N=2-5$ can be related to the difference in M.

At $T=4.2$ K and $H_{\text{ext}}=80$ kOe ($H_{\text{ext}}/T=19$ kOe/K), the hyperfine field is considered to be almost saturated. Since the saturation hyperfine field is generally assumed to be proportional to the magnitude of the localized magnetic moment associated with the impurity, the dependence of H_{hf} on N reflects the dependence of the localized moment on N. Consequently, in the Ir-Pt(Fe) system the magnitude

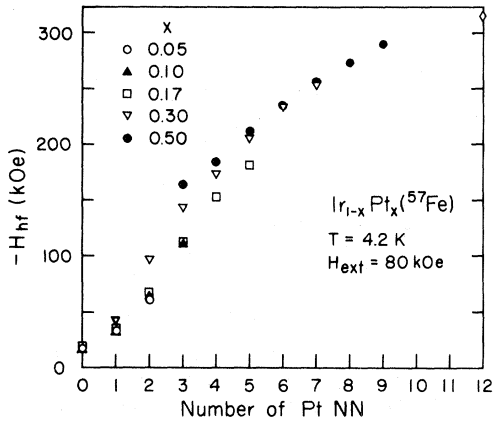

FIG. 4. Hyperfine field of ^{57}Fe in $Ir_{1-x}Pt_x$ hosts at 4.2 K and 80 kOe as a function of the number of Pt nearest neighbors. The result for $N=12$ is derived from the data on Pt(^{57}Fe) of Ref. 11.

of localized moment increases continuously with the number of NN Pt atoms.

This conclusion is contrary to the previous works with Nb-Mo(Fe),[2-4] which support the discontinuous formation of localized moment. The origin of this opposition can be found in the different magnetic character of Fe impurities in the host elements. Ir(Fe) is more magnetic than Nb(Fe) for the following reason: The magnetic character of the latter is simple nonmagnetic and H_{hf} of ^{57}Fe in Nb is $+1$ kOe at $T=4.2$ K and $H_{\text{ext}}=60$ kOe.[19] Whereas, dilute alloy Ir(Fe) is an LSF system and H_{hf} of ^{57}Fe in Ir is -15 kOe at 4.2 K and 80 kOe.[10] Besides, it is well known that Fe impurity in Pt makes up a giant magnetic moment by the polarization of near-neighbor Pt atoms.[11,13] In this case, the fluctuation in spin density in the d band of Pt metal plays an important role. Therefore, it is likely that in Ir-Pt(Fe) alloy the spin polarization of the host promotes the continuous formation of localized moment of Fe impurities in the LSF state. The appreciable contribution of NNN Pt atoms to H_{hf} also supports the polarization of NN shells. A similar result has been reported for binary alloy Fe-V with bcc structure.[18] For this sytem, the moment per Fe as a function of the number of Fe NN's increases almost linearly, but has a slight S-like deviation.

The temperature and field dependence of H_{hf} give more detailed information on the formation of localized moment. For this purpose, extensive measurements were carried out with the hosts of $Ir_{0.9}Pt_{0.1}$ and $Ir_{0.5}Pt_{0.5}$. In Fig. 5, $H_{\text{hf}}(N)$ of ^{57}Fe in these two hosts is plotted as a function of H_{ext}/T, where H_{ext} is fixed at 80 kOe. The figure shows that the curves of H_{hf} shift depending on N. The data of $Ir_{0.5}Pt_{0.5}$ were fitted to a Brillouin function

$$H_{\text{hf}}=H_{\text{sat}}B_J(\mu H_{\text{ext}}/kT)\ , \qquad (1)$$

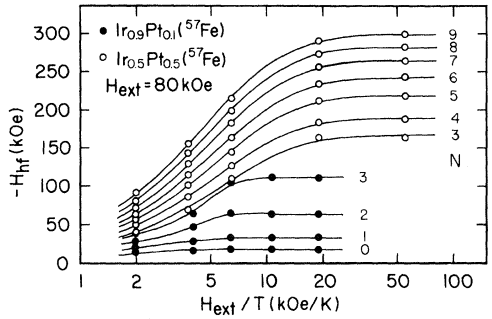

FIG. 5. Behavior of hyperfine field of ^{57}Fe impurities with different number of Pt nearest neighbors as a function of H_{ext}/T, where $H_{ext}=80$ kOe. Solid lines for $Ir_{0.5}Pt_{0.5}$ are the fits to Brillouin functions, and for $Ir_{0.9}Pt_{0.1}$ are drawn only as a visual aid.

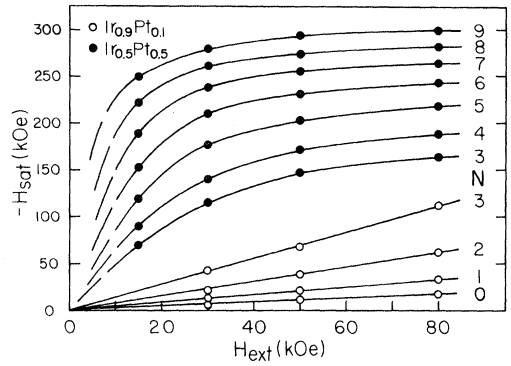

FIG. 6. Saturation hyperfine field of ^{57}Fe impurities with different number of Pt nearest neighbors as a function of external field. Temperature is 1.5 K.

where H_{sat} is the saturation hyperfine field for large values of H_{ext}/T, $\mu = gJ\mu_B$ is the magnetic moment of Fe impurity, and g is assumed to be 2.17, referring the value for Pt(^{57}Fe).[11] Least-square curves are drawn by solid lines in the figure. The data of $N=9$ are well fitted with parameters $H_{sat}=298.4$ kOe and $J=2.27$, indicating that the magnetic moment associated with Fe atom behaves as a free giant moment of $\mu=4.93\mu_B$. This value is compatible with $6.46\mu_B$ for Fe in Pt.[11] This fact confirms that the giant moment of $N=9$ is certainly caused by the polarization of near-neighbor shells. As N decreases, the magnitude of magnetic moment decreases to $3.41\mu_B$ ($N=3$), but the normalized χ square increases.

The results of $Ir_{0.9}Pt_{0.1}$ could not be described by the Brillouin function. The solid lines are drawn only as an aid and do not represent any theoretical function. The monotonic behavior of the curve for $N=0$ is consistent with our previous result of Ir(^{57}Fe),[9] where H_{hf} already saturates for $H_{ext}/T > 2$ kOe/K.

It is remarkable that H_{hf} curves of $N=3$ for these two samples show different behaviors. As to $Ir_{0.9}Pt_{0.1}$, the curve approaches to a constant faster than that for $Ir_{0.5}Pt_{0.5}$ and the saturation hyperfine field is much suppressed. This difference is undoubtedly related to the expected value of the number of NNN Pt atoms $\bar{M}$, 0.6 for the former and 3.0 for the latter.

It is well known that for Kondo and LSF systems the saturation hyperfine field H_{sat} depends on the external field.[9,20–24] In Fig. 6, we plot H_{hf} obtained at 1.5 K as a function of H_{ext} (15–80 kOe). Referring to Fig. 5, H_{hf} under the conditions are considered to be sufficiently close to H_{sat}, and reveal nicely the different dependence of $H_{sat}(N)$ on H_{ext}. As N decreased, higher H_{ext} is required to achieve saturation of H_{sat} curves of $Ir_{0.5}Pt_{0.5}$. For $Ir_{0.9}Pt_{0.1}$, H_{sat} of $N=3$–0 does not saturate but increases linearly with H_{ext}, i.e., the saturation of magnetic moment becomes difficult for the Fe impurity with few NN Pt atoms. The linear behavior of H_{sat} for $Ir_{0.9}Pt_{0.1}$ closely resembles that of LSF system Tc(Fe)[9] and of Kondo system Cu(Fe).[20,21] In the case of Cu(Fe), the linear dependence was qualitatively explained as follows: Since Cu(Fe) has a high Kondo temperature $T_K=28$ K, it is not possible to complete the breaking up of the spin compensation state with the available field strength.

Unfortunately, to the authors' knowledge, appropriate prediction based on the LSF model for the dependence of H_{sat} on H_{ext} has not been reported. As to the Kondo systems of Mo(Fe),[22] Rh(Fe),[23] and Ag(Fe),[24] the field dependence of H_{sat} at $T=0$ K has been analyzed using the Ishii theory[25] on the singlet ground state, which is expressed as[22]

$$H_{sat}(H_{ext}) = H_{sat}(\infty)\mu H_{ext}/[(\mu H_{ext})^2 + (kT_K)^2]^{1/2} \quad . \tag{2}$$

Comparison between the present results and Eq. (2) suggests that T_K increases with decreasing N. However, the uncertainty in the values of $H_{sat}(\infty)$ and μ does not allow the accurate estimation of T_K.

For the component of $N=3$, the behavior of $H_{sat}(H_{ext})$ of $Ir_{0.9}Pt_{0.1}$ is inconsistent with that of $Ir_{0.5}Pt_{0.5}$. The different behavior in $H_{sat}(H_{ext})$ as well as in $H_{hf}(H_{ext}/T)$ indicates that the magnetic character (or T_{sf}) is influenced by the NNN Pt atoms. The values of H_{sat} for $N=3$, however, seem to be asymptotic at $H_{ext}=\infty$. By comparing two curves with Eq. (2), one can say that the LSF (or Kondo) temperature of Fe impurities characterized by $N=3$ and $\bar{M}=3.0$ ($Ir_{0.5}Pt_{0.5}$) is considerably lower than that characterized by $N=3$ and $\bar{M}=0.6$ ($Ir_{0.9}Pt_{0.1}$).

IV. SUMMARY

Mössbauer investigation of ^{57}Fe impurities in Ir-Pt alloys has revealed that the spectra of the alloys can-

not be explained by the model of discontinuous formation of localized magnetic moment. Instead, analysis of the distribution of hyperfine field showed that the saturation hyperfine field of ^{57}Fe increases smoothly with increasing the number of NN Pt atoms. Besides, an appreciable contribution of NNN Pt atoms to the hyperfine field was observed.

The dependences of hyperfine field on temperature and on external field were studied for the hosts of $Ir_{0.9}Pt_{0.1}$ and $Ir_{0.5}Pt_{0.5}$. For the former, the saturation hyperfine field of Fe impurities with 0–3 Pt NN's increases in proportion to the external field up to 80 kOe. This property closely resembles that of LSF system Tc(Fe)[9] and of Kondo system Cu(Fe).[20,21] The behavior of $H_{hf}(H_{ext}/T)$ and of $H_{sat}(H_{ext})$ as a function of the number of Pt NN's suggests a smooth transition of the magnetic character of Fe impurities. As to Fe impurities with 9 Pt NN's, $H_{hf}(H_{ext}/T)$ follows closely a Brillouin function with a large magnetic moment of $\mu = 4.93\mu_B$, which is attributed to the polarization of near-neighbor Pt atoms. In the case of Fe impurities with 3 Pt NN's, the LSF temperature is considerably affected by the NNN configuration. Unfortunately, the shift in T_{sf} could not be estimated from the present data due to the absence of appropriate theoretical prediction.

These experimental results lead to the conclusion that the magnetic moment associated with Fe impurities in Ir-Pt hosts is formed continuously with the aid of polarization of Pt atoms in nearest- and next-nearest neighbor shells. This conclusion is in basic agreement with the prediction of van der Rest's theory.[7] In summary, we can say that the magnetic state of Fe impurities in Ir-Pt hosts changes smoothly from the LSF state to the giant moment state depending on the local environment.

ACKNOWLEDGMENTS

The authors acknowledge the help of Dr. Y. Muraoka and K. Kanoda with the sample preparation. We are indebted to N. Hosoito and Dr. T. Mukoyama for their assistance with the computer analysis. The suggestions by Dr. M. Shiga have been much appreciated. This work was supported by the Grant-in-Aid for Scientific Research from the Japanese Ministry of Education.

[1]For a general reference to earlier literature, see L. W. Garland and A. Gonis, in *Magnetism in Alloys,* edited by J. T. Waber and P. A. Beck (Metallurgical Society of A. I. M. E., New York, 1972), p. 78.
[2]H. Nagasawa and N. Sakai, J. Phys. Soc. Jpn. 27, 1150 (1969).
[3]L. J. Swartzendruber, Int. J. Magn. 2, 129 (1972).
[4]H. Maletta and K. R. P. M. Rao, Int. J. Magn. 3, 5 (1973).
[5]M. P. Maley, R. D. Taylor, and D. J. Erickson, J. Appl. Phys. 52, 1673 (1981).
[6]V. Jaccarino and L. R. Walker, Phys. Rev. Lett. 15, 258 (1965).
[7]J. van der Rest, J. Phys. F 8, 1263 (1978).
[8]N. Rivier and V. Zlatic, J. Phys. F 2, L99 (1972).
[9]T. Takabatake, H. Mazaki, and T. Shinjo, Phys. Rev. B 21, 2706 (1980).
[10]T. Takabatake, H. Mazaki, and T. Shinjo, Bull. Inst. Chem. Res., Kyoto Univ. 59, 20 (1981).
[11]M. P. Maley, R. D. Taylor, and J. L. Thompson, J. Appl. Phys. 38, 1249 (1967).
[12]M. Scherg, E. R. Seider, F. J. Litterst, W. Gierisch, and G. M. Kalvius, J. Phys. (Paris) 35, C6-527 (1974).
[13]T. H. Geballe, B. T. Matthias, A. M. Clogston, H. J. Williams, R. C. Sherwood, and J. P. Maita, J. Appl. Phys. 37, 1181 (1966).
[14]M. Hansen, *Constitution of Binary Alloys* (McGraw-Hill, New York, 1958), p. 871.
[15]B. Window, J. Phys. E 4, 401 (1971).
[16]J. Hesse and A. Rübartsch, J. Phys. E 7, 526 (1974).
[17]S. J. Campbell, P. E. Clark, and T. J. Hicks, J. Phys. F 6, 249 (1976).
[18]M. Shiga and Y. Nakamura, J. Phys. F 8, 177 (1978).
[19]T. A. Kitchens, W. A. Steyert, and R. D. Taylor, Phys. Rev. 138, A467 (1965).
[20]R. B. Frankel, N. A. Blum, B. B. Schwartz, and D. J. Kim, Phys. Rev. Lett. 18, 1051 (1967).
[21]P. Steiner, S. Hüfner, and W. v. Zdrojewski, Phys. Rev. B 10, 4704 (1974).
[22]M. P. Maley and R. D. Taylor, Phys. Rev. B 1, 4213 (1970).
[23]P. E. Clark, Solid State Commun. 12, 469 (1973).
[24]P. Steiner and S. Hüfner, Phys. Rev. B 12, 842 (1975).
[25]H. Ishii, Prog. Theor. Phys. 43, 578 (1970).